



Contents lists available at ScienceDirect

Chinese Chemical Letters

journal homepage: [www.elsevier.com/locate/cclet](http://www.elsevier.com/locate/cclet)

# DNA walker induced “signal on” fluorescence aptasensor strategy for rapid and sensitive detection of extracellular vesicles in gastric cancer

Gaojian Yang<sup>a,1</sup>, Zhiyang Li<sup>c,1</sup>, Rabia Usman<sup>a</sup>, Zhu Chen<sup>b,d,e</sup>, Yuan Liu<sup>d,e,\*</sup>, Song Li<sup>d,e</sup>, Hui Chen<sup>d,e</sup>, Yan Deng<sup>d,e,\*</sup>, Yile Fang<sup>a,\*</sup>, Nongyue He<sup>a,b,\*</sup>

<sup>a</sup> State Key Laboratory of Digital Medical Engineering, School of Biological Science and Medical Engineering, Southeast University, Nanjing 210096, China

<sup>b</sup> Hunan Key Laboratory of Biomedical Nanomaterials and Devices, Hunan University of Technology, Zhuzhou 412007, China

<sup>c</sup> Department of Clinical Laboratory, the Affiliated Drum Tower Hospital of Nanjing University Medical School, Nanjing 210008, China

<sup>d</sup> Institute of Cytology and Genetics, School of Basic Medical Sciences, Hengyang Medical School, University of South China, Hengyang 421001, China

<sup>e</sup> Institute for Future Sciences, University of South China, Changsha 410000, China

## ARTICLE INFO

### Article history:

Received 20 February 2024

Revised 19 April 2024

Accepted 27 April 2024

Available online 29 April 2024

### Keywords:

Extracellular vesicles

Aptamer

Streptavidin magnetic beads

Nt.BbvCI

Detection

## ABSTRACT

The extracellular vesicles show great potential as a noninvasive biomarker for the early detection of cancer. Hence, there is an urgent requirement to create biosensors that are time-saving, simple, and easily scalable in order to accomplish rapid, sensitive, and quantitative detection of extracellular vesicles. In this study, we present a self-propelled DNA walker powered by endonuclease Nt.BbvCI, which enables the development of a “signal on” sensing platform for the rapid and highly sensitive detection of extracellular vesicles. The DNA motor employed tracks made of streptavidin magnetic beads, which consisted of substrate strands labeled with fluorescein and motor strands locked by aptamers. The aptamer recognition of the target protein on extracellular vesicles unlocked the motor strand, initiating the DNA motor process. After replacing the optimal buffer solution containing the endonuclease Nt.BbvCI, the motor strands autonomously moved along the streptavidin magnetic beads track, continuously releasing fluorescent molecules and producing detectable fluorescence signals. Under optimal conditions, the detection range was from  $2 \times 10^4$  particles/mL to  $2 \times 10^9$  particles/mL, with a detection limit of  $2.9 \times 10^3$  particles/mL, demonstrating excellent selectivity. This method has demonstrated good selectivity in different tumor-derived extracellular vesicles and performs well in complex biological samples. The ability to effectively analyze surface proteins of extracellular vesicles in a short period of time gives our DNA walker a tremendous potential for developing simple and cost-effective clinical diagnostic devices.

© 2024 Published by Elsevier B.V. on behalf of Chinese Chemical Society and Institute of Materia Medica, Chinese Academy of Medical Sciences.

According to the global cancer statistics in 2020 [1], there were approximately 1.09 million new cases of stomach cancer and 780,000 deaths. Unfortunately, most patients are only diagnosed with middle or late-stage gastric cancer when they experience significant symptoms such as loss of appetite, indigestion, and abdominal pain, with a 5-year survival rate less than 10% after treatment [2]. In the current clinical diagnosis of gastric cancer, endoscopy and tissue biopsy are invasive procedure, while imaging diagnosis has low sensitivity for early diagnosis [3–5]. Therefore, there is an urgent demand to establish reliable detection techniques for precise early diagnosis of gastric cancer.

Extracellular vesicles are secreted by cells, ranging in size from 30 nm to 200 nm, and are present in various body fluids, including blood [6], urine [7], lymphatic fluid [8], saliva [9], cerebrospinal fluid [10], and pleural/peritoneal fluid [11,12]. Extracellular vesicles carry abundant substances such as proteins and nucleic acids, which are consistent with the parent cells, and can transmit biological information to recipient cells through cell membrane fusion [13–15]. Recent reports indicate that tumor-derived extracellular vesicles are involved in tumor metastasis [16–18], progression [19], and immune regulation [20,21]. Given their abundance in body fluids, non-invasive nature, ability for real-time assessment, and stable properties, extracellular vesicles (EVs) are considered to have great potential in cancer liquid biopsy [22,23].

Currently, methods for quantifying extracellular vesicles, such as nano-flow cytometry (nFCM) [24–26] and nanoparticle tracking analysis (NTA) [27,28], have low detection sensitivity and poor specificity [29]. Although the sensitivity and specificity of further

\* Corresponding authors.

E-mail addresses: [gxliuyuan@163.com](mailto:gxliuyuan@163.com) (Y. Liu), [hndengyan@126.com](mailto:hndengyan@126.com) (Y. Deng), [fang1le@qq.com](mailto:fang1le@qq.com) (Y. Fang), [nyhe1958@163.com](mailto:nyhe1958@163.com) (N. He).

<sup>1</sup> These authors contributed equally to this work.

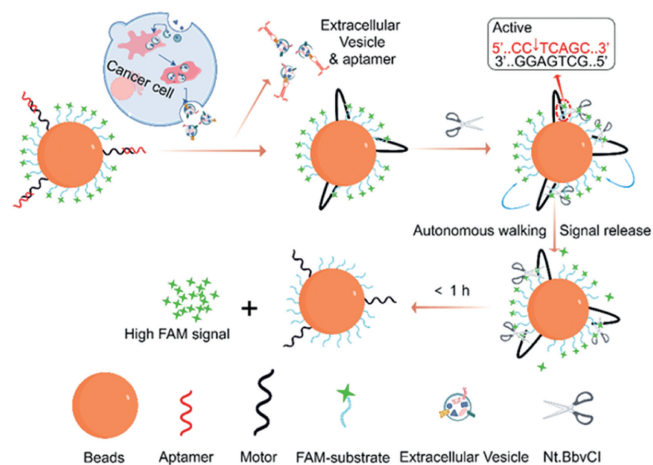


Fig. 1. Schematic illustration of the principle of the DNA walker.

developed enzyme-linked immunosorbent assay (ELISA) [30,31] and colorimetric detection [32,33] have been improved, they are still unsatisfactory. Amplification strategies such as nanomaterials [34–37], rolling circle amplification (RCA) [38–40], and hybridization chain reaction (HCR) [41–43] have also been used for fluorescence detection [44,45], which greatly improves the detection sensitivity. Nevertheless, there is a need to enhance their quenching efficiency and reduce the incubation time. Recently, microfluidics [46,47], surface plasmon resonance (SPR) [48,49], and digital PCR [50,51] platforms have been developed for the detection of extracellular vesicles. However, the expensive instruments and complex engineering designs hinder their wider application. According to the work of Yu *et al.* [52], although the nanoparticle-conjugated signal probe can effectively quench the signal, the inflexibility of the detection system makes it difficult to achieve optimal enzyme activity. As a result, the incubation time for this platform is as long as 3 h, which is also difficult to integrate it into a rapid detection platform [53]. Therefore, there is a need to develop a rapid automated detection platform for tumor-derived extracellular vesicles.

In this paper, we propose a DNA motor [54,55] with magnetic beads as tracks, which can specifically respond to tumor-derived extracellular vesicles through aptamer-based molecular recognition. We firstly immobilized the biotinylated substrate strand labeled with fluorescein and the motor strand locked by aptamers [56] onto magnetic beads through biotin-streptavidin affinity. In the presence of tumor-derived extracellular vesicles, a specific surface protein-aptamer binding event was triggered. After replacing the optimal buffer solution containing the endonuclease Nt.BbvCI, the motor strand autonomously moves along the magnetic bead track, releasing fluorescent molecules and generating detectable fluorescence signals. The fluorescence gradually increases during the walking process, resulting in signal amplification. It is worth noting that we can flexibly change the detection buffer during the process to make it more suitable for enzyme reactions, greatly reducing the detection time. Additionally, the detection platform is potentially automated since it is based on magnetic beads.

DNA walker triggered by extracellular vesicles was revealed in Fig. 1 (drawn by Figdraw). Substrate strands and motor strands were immobilized on the beads in a certain proportion, which served on the buttress of the three-dimensional tracks. The locking strands (the specific target-recognized aptamers) were immobilized on the one end of the motor strands by hybridization. Mucin-1 (MUC1) aptamers can specifically recognize the surface protein MUC1 of extracellular vesicles derived from gastric cancer cells were selected as the locking strands in this work. The aptamers as locking strands preferentially integrated to protein MUC1 on the

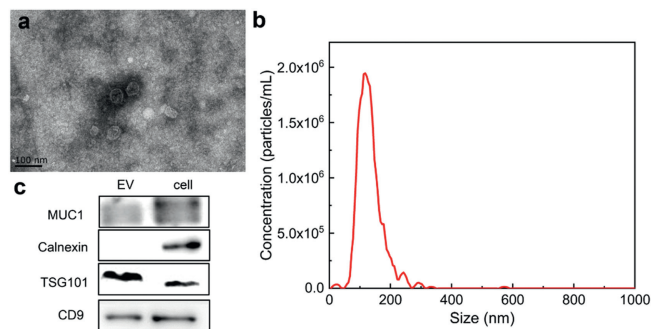
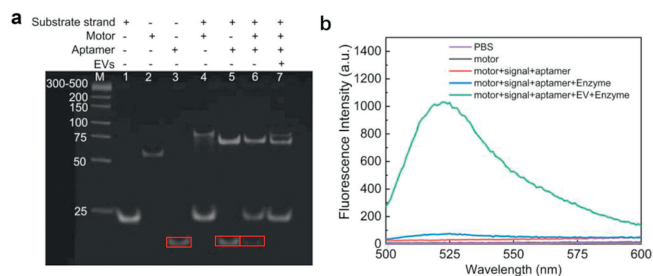


Fig. 2. Characterization of tumor-derived extracellular vesicles. (a) TEM image of purified extracellular vesicles derived from MGC-803 cells. (b) Size distribution of extracellular vesicles obtained by NTA. (c) WB analysis of CD9, TSG101, MUC1 and Calnexin protein on MGC-803 cell lysates and extracellular vesicles derived from MGC-803 cell.

extracellular vesicles to release the motor strands in the presence of gastric cancer extracellular vesicles. The released motor strands hybridized with the substrate strands on the magnetic beads result in the hybridization strands containing the sequence sites recognized by restriction endonuclease Nt.BbvCI and cleaved the substrate strands. The motor strand would combined with another substrate strand and walked autonomously and persistently along the magnetic bead track actuated by Nt.BbvCI. There was a fluorescent molecule would be released by cleaved substrate strands as a result of one step of motor strands, then the fluorescence was emitted. Thus, the displacement of DNA walker can be able to real-time monitored by fluorescence detection, the fluorescence intensity was positively correlated with the amount of kinematic strands released by extracellular vesicles. Conversely, in the absence of gastric cancer extracellular vesicles, aptamers could not be dissociated from the motor strands, resulting in the inability of the motor strands bind to the substrate strands for digestion reaction, therefore, the FAM fluorophore cannot be released to obtain the fluorescent signal.

Gastric tumor-derived extracellular vesicles were regarded as the detection target, therefore, we performed a series of characterization of extracellular vesicles extracted by differential ultracentrifugation. According to the recommendations of MISEV2018, the extracellular vesicles were determined by NTA, transmission electron microscope (TEM) and Western blot (WB), separately. As shown in Fig. 2a, the morphology of extracellular vesicles which demonstrated classically cup-shaped with phospholipid bilayer was observed by TEM, in accordance with previous reports. The size distribution of extracellular vesicles was characterized by NTA (Fig. 2b), the range of size was in 30–200 nm, and the average was approximately 120 nm. Besides, the signature proteins cluster of differentiation 9 (CD9) and tumor susceptibility genes 101 (TSG101) of extracellular vesicles, the specific proteins MUC1 of gastric tumor-derived extracellular vesicles, and the negative protein calnexin were also authenticated. CD9, TSG101 and MUC1 were all positive in gastric tumor-derived extracellular vesicles, which were described in Fig. 2c, indicating the extracted samples were gastric tumor-derived extracellular vesicles.

To evaluate the feasibility of our DNA walker platform, we employed native polyacrylamide gel electrophoresis (PAGE) to characterize the hybridization of DNA complexes. As shown in Fig. 3a, the bands in lanes 1–3 represent substrate strands, DNA motors, and aptamers, respectively. Comparing lanes 1, 2, and 4, a new band appeared at around 80 bp in lane 4, indicating the hybridization of substrate strands with DNA motors at room temperature. When examining lanes 2, 3, and 5, it becomes evident that a new band materialized at approximately 75 bp in lane 5, signifying the bind-



**Fig. 3.** Feasibility test of extracellular vesicles detection. (a) Native PAGE images showing the strand cleavage and displacement. (b) The fluorescence spectra of the proposed systems obtained in the presence of different reagents.

ing of aptamers to DNA motors. When incubated with substrate strands after the annealing of aptamers and DNA motors, no band was observed at around 80 bp in lane 6, indicating no hybridization between substrate strands and DNA motors. However, in the presence of extracellular vesicles (lane 7), aptamers were bound to the EVs (removing the complex by using a 50 kDa ultrafiltration membrane), leading to the release of DNA motors and their hybridization with substrate strands, resulting in the appearance of a band at around 80 bp. These results preliminarily demonstrate the feasibility of the DNA walker platform with aptamer-closed DNA motors.

In order to validate the suitability of the DNA walker platform for fluorescence detection, fluorescence assay was employed as a subsequent verification step. Initially, the substrate strands and motors+MUC1 aptamer complexes were separately immobilized on magnetic beads using biotin-streptavidin affinity. Subsequently, Nt.BbvCI (control group) and Nt.BbvCI + extracellular vesicles (experimental group) were added to the magnetic beads containing motors+MUC1 aptamer complexes. After incubation, the supernatant was subjected to magnetic separation for fluorescence detection to assess the cleavage of substrate strands and the subsequent release of fluorescence signal. As depicted in Fig. 3b, a significant fluorescence signal was only observed in the presence of extracellular vesicles. This indicates that upon competitive binding of extracellular vesicles with MUC1 aptamer, the motors were released, hybridized with substrate strands, recognized by Nt.BbvCI, resulting in the cleavage of substrate strands and subsequent release of fluorescence signal probe. Hence, this further validates the feasibility of this sensing system.

In order to determine the optimal amounts of streptavidin magnetic beads and endonuclease under fixed conditions of substrate strands and complex of DNA motors and aptamers, optimization of the conditions is required. The volume of magnetic beads directly affects the binding efficiency. When the volume of streptavidin magnetic beads is increased from 10  $\mu$ L to 20  $\mu$ L, the fluorescence signal significantly increases (Fig. S1a in Supporting information). This indicates that the fixed amount of substrate strands and the complex of DNA motors and aptamers on the streptavidin magnetic beads increases. After activating the DNA walker, the number of substrate strands available for cleavage increases, resulting in the release of more fluorescence signal probes. When the volume of streptavidin-coated magnetic beads increased from 20  $\mu$ L to 60  $\mu$ L, the substrate strands and the complex of DNA motors and aptamers were completely immobilized, resulting in the saturation of fluorescence signal and reaching a stable state. Therefore, 20  $\mu$ L was selected as the optimum quantity of magnetic beads. Likewise, the dosage of restriction endonuclease was optimized (Fig. S1b in Supporting information). With an increase in the dosage of restriction endonuclease from 1 U to 3 U, more substrate strands can be cleaved simultaneously after activating the DNA walker, thereby increasing the fluorescence signal. Increasing the dosage of restric-

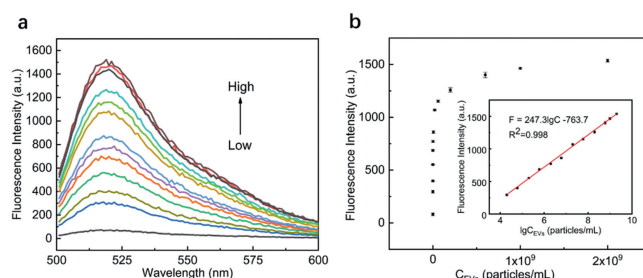


**Fig. 4.** Detection performance under optimal experimental conditions. (a) The fluorescence spectrogram. (b) The scatter plot of fluorescence intensity (the inline diagram is a linear regression between the logarithm of extracellular vesicles concentration and fluorescence intensity).

tion endonuclease from 3 U to 7 U did not result in a significant enhancement of the fluorescence signal. This indicates that the saturation point was reached when the amount of restriction endonuclease used was 3 U.

Since incubation temperature and time were both essential for enzymatic reactions, the DNA walker was operated in solution at 4, 25, 37 and 45  $^{\circ}$ C, 10–80 min respectively. DNA motors exhibit high operational efficiency as they run in solutions at different temperatures. The enzyme activity and fluorescence signal generated by the DNA motors are highest at 37  $^{\circ}$ C, indicating their optimal performance (Fig. S2a in Supporting information). The efficiency of motion significantly decreases when the working temperature is higher or lower than 37  $^{\circ}$ C. As shown in Fig. S2b (Supporting information), the fluorescence signal gradually increased as the incubation time ranged from 10 min to 50 min. However, there was no significant increase in the fluorescence signal after 50 min of incubation. Thus, the optimal incubation temperature and time were 37  $^{\circ}$ C and 50 min respectively.

Subsequently, we further optimized the detection performance of the reaction under different buffers. As shown in Fig. S3 (Supporting information), the maximum fluorescence signal of Nt.BbvCI is observed in NEBuffer, therefore NEBuffer is chosen as the optimal buffer of Nt.BbvCI for subsequent experiments. The spatial hindrance and efficiency of DNA motors movement are directly affected by the different lengths of DNA motors and the ratio of motor to substrate strand, as they move on the surface of streptavidin magnetic beads. According to Fig. S4a (Supporting information), the maximum fluorescence signal emerged as the motor length was 45 nt, indicating that the optimum motor length is 45 nt. In addition, we have recorded fluorescence results of different motor: substrate strand ratio over the reaction time (Fig. S4b in Supporting information). The fluorescence signal gradually rises primitively with the motor: substrate strand ratio from 1:1 to 1:7. As the motor: substrate strand ratio increases from 1:7 to 1:9, the fluorescence signal slightly decreases. This may be due to the high density of substrate strands, which creates spatial hindrance for the hybridization between motors and substrate strands, resulting in a decrease in the hybridization efficiency between substrate strands and DNA motors. Thus, ratio of motor and substrate strand is 1:7 for DNA walker were employed for subsequent experiments.

A series of concentrations of standard extracellular vesicles was investigated into the DNA walker platform for the linear dependence and detection limit. As shown in Fig. 4a, there is a strong fluorescent signal at 520 nm with gradual increase upon growing the extracellular vesicles concentration, indicating that the more extracellular vesicles concentration caused more cleaving reactions. The circumstantial relativity between the fluorescent intensity and the amount of extracellular vesicles was described in Fig. 4b. Distinctly, extracellular vesicles could be detected immediately in the range from  $2 \times 10^4$  particles/mL to  $2 \times 10^9$  particles/mL. Moreover, A

good linear dependence is established between the variation of the fluorescent intensity and logarithm of extracellular vesicles concentration as:  $F = 247.31\lg C - 763.7$  ( $R^2 = 0.998$ ), where  $F$  is the variation of the fluorescent intensity. The limit of detection (LOD) was calculated to be  $2.9 \times 10^3$  particles/mL. These results verified a great sensitivity of the DNA walker for the trace quantity detection of extracellular vesicles.

The specificity of the DNA-walker was investigated by different originations of EVs, the fluorescence signal of MGC-803 extracellular vesicles was much higher than human gastric mucosal epithelial cells (GES-1) extracellular vesicles, which is reproducible at different concentrations of EVs:  $2 \times 10^6$ ,  $2 \times 10^7$  and  $2 \times 10^8$  particles/mL, demonstrating the high specificity of the proposed DNA walker (Fig. S5 in Supporting information).

Extracellular vesicles-free fetal bovine serum (FBS) with the addition of tumor extracellular vesicles was used to analyze the practicability of DNA-walker. Gastric tumor MGC-803 extracellular vesicles and epithelium GES-1 extracellular vesicles were determined in multiple dilution of FBS, obviously described in Fig. S6 (Supporting information), the sensor had a favorable distinction between gastric cancer cell MGC-803 and EVs of epithelial cell GES-1 under conditions below 1/30 dilution of FBS. Therefore, the proposed DNA walker was feasible for determining extracellular vesicles in biological environment.

In this work, we developed a DNA walker detection platform that utilizes tumor-derived extracellular vesicles to initiate a reaction. In the presence of a restriction endonuclease, the substrate strands labeled with fluorescein are rapidly cleaved, resulting in the release of fluorescent molecules and the generation of a fluorescence signal. The advantages of our work are mainly reflected in two aspects: (1) The endonuclease we used for cleavage of the DNA has superior stability and reaction kinetics under optimized conditions, which is beneficial for improving sensitivity. (2) The DNA walker detection platform based on streptavidin magnetic beads that we proposed in our work has a controllable incubation time within 1 hour and has the potential for further development into an automated detection system. After activation of the DNA walker, the fluorescently labeled DNA strand is cleaved, resulting in fluorescence recovery. The obtained extracellular vesicles concentration is positively correlated with the fluorescence increment. The proposed method offers a very low detection limit of approximately  $2.9 \times 10^3$  particles/mL and a wide dynamic detection range. In addition, this strategy exhibits excellent selectivity and specificity in complex biological samples, and has a short detection time. With these advantages, we anticipate that this assay has great potential for the development of a rapid, cost-effective, sensitive, and selective extracellular vesicles characterization platform in future clinical applications.

### Declaration of competing interest

The authors declare that they have no known competing financial interests or personal relationships that could have appeared to influence the work reported in this paper.

### CRediT authorship contribution statement

**Gaojian Yang:** Writing – review & editing, Writing – original draft, Formal analysis, Data curation. **Zhiyang Li:** Validation, Methodology, Investigation, Data curation, Conceptualization. **Rabia Usman:** Resources, Data curation, Conceptualization. **Zhu Chen:** Investigation, Formal analysis. **Yuan Liu:** Writing – review & editing, Visualization, Validation, Conceptualization. **Song Li:** Validation, Supervision, Conceptualization. **Hui Chen:** Resources, Data curation, Conceptualization. **Yan Deng:** Visualization, Supervision,

Project administration, Methodology, Funding acquisition, Conceptualization. **Yile Fang:** Visualization, Validation, Supervision, Data curation. **Nongyue He:** Writing – review & editing, Supervision, Resources, Project administration, Funding acquisition, Conceptualization.

### Acknowledgments

This research was supported financially by the National Natural Science Foundation of China (NSFC, Nos. 62071119 and 62075098) the National Key Research and Development Program of China (Nos. 2017YFA0205301 and 2018YFC1602905).

### Supplementary materials

Supplementary material associated with this article can be found, in the online version, at doi:10.1016/j.ccllet.2024.109930.

### References

- [1] H. Sung, J. Ferlay, R.L. Siegel, et al., *CA Cancer J. Clin.* 71 (2021) 209–249.
- [2] M. Orditura, G. Galizia, V. Sforza, et al., *World J. Gastroenterol.* 20 (2014) 1635–1649.
- [3] V. Pasechnikov, S. Chukov, E. Fedorov, et al., *World J. Gastroenterol.* 20 (2014) 13842–13862.
- [4] Z. Guo, B. Jin, Y. Fang, et al., *Chin. Chem. Lett.* 35 (2024) 108528.
- [5] C.L. Cai, T. Wang, X. Han, et al., *Chin. Chem. Lett.* 33 (2022) 1963–1969.
- [6] J.D. Klein, X.H. Wang, *Am. J. Physiol. Renal. Physiol.* 315 (2018) 1542–1549.
- [7] H. Zhou, P.S.T. Yuen, T. Pisitkun, et al., *Kidney Int.* 69 (2006) 1471–1476.
- [8] S.S. Garcia, E.P. Ximenez, J. Munoz, et al., *Methods Mol. Biol.* 2265 (2021) 345–359.
- [9] Y. Ogawa, A.M. Kanai, Y. Akimoto, et al., *Biol. Pharm. Bull.* 31 (2008) 1059–1062.
- [10] N. Hayashi, H. Doi, Y. Kurata, et al., *Neurosci. Res.* 160 (2020) 43–49.
- [11] T. Hiroyuki, M. Akihisa, S. Akira, et al., *Anticancer Res.* 38 (2018) 6707.
- [12] H.M. Nazri, M. Imran, R. Fischer, et al., *Fertil. Steril.* 113 (2020) 364–373.
- [13] Y.M. Tavakkoli, A. Tukova, Y. Wang, *Nanoscale* 14 (2022) 15242–15268.
- [14] J. Zhang, Y. Zhu, M. Guan, et al., *Nanoscale* 14 (2022) 8995–9003.
- [15] Y. Jia, L. Yu, T. Ma, et al., *Theranostics* 12 (2022) 6548–6575.
- [16] S. Bai, Z. Wang, M. Wang, et al., *Front. Cell Dev. Biol.* 10 (2022) 752818.
- [17] B. Yin, J. Ni, C.E. Witherell, et al., *Theranostics* 12 (2022) 207–231.
- [18] L. Zhang, L. Xu, Y. Wang, et al., *Chin. Chem. Lett.* 34 (2023) 4089–4095.
- [19] H. Wang, Y. You, X. Zhu, *Front. Oncol.* 12 (2022) 887518.
- [20] J. Zou, H. Peng, Y. Liu, *Front. Immunol.* 12 (2021) 757674.
- [21] T. Yin, Y. Liu, W. Ji, et al., *Theranostics* 13 (2023) 1264–1285.
- [22] A. Slomka, B. Wang, T. Mocan, et al., *Theranostics* 12 (2022) 5836–5855.
- [23] L. Wu, Y. Wang, X. Xu, et al., *Chem. Rev.* 121 (2021) 12035–12105.
- [24] S. Zhu, L. Ma, S. Wang, et al., *ACS Nano* 8 (2014) 10998–11006.
- [25] Y. Tian, L. Ma, M. Gong, et al., *ACS Nano* 12 (2018) 671–680.
- [26] Y. Tian, M. Gong, Y. Hu, et al., *J. Extracell. Vesicles* 9 (2020) 1697028.
- [27] T.C. Gercel, S. Atay, R.H. Tullis, et al., *Anal. Biochem.* 428 (2012) 44–53.
- [28] C.Y. Soo, Y. Song, Y. Zheng, et al., *Immunology* 136 (2012) 192–197.
- [29] M. Hussain, X. Liu, J. Zou, et al., *Chin. Chem. Lett.* 33 (2022) 1885–1888.
- [30] J. Lee, H. Kim, Y. Heo, et al., *Analyst* 145 (2020) 157–164.
- [31] H. Zhao, E. Su, L. Huang, et al., *Chin. Chem. Lett.* 33 (2022) 743–746.
- [32] L. Ning, Y. Zhou, Y. Xie, et al., *Anal. Sci. Technol.* 14 (2023) 5.
- [33] Y. Liu, T. Li, G. Yang, et al., *Chin. Chem. Lett.* 33 (2022) 1913–1916.
- [34] Y. Fang, Y. Wang, L. Zhu, et al., *Chin. Chem. Lett.* 34 (2023) 108092.
- [35] J. Liu, R. Wang, H. Zhou, et al., *Nanoscale* 14 (2022) 10286–10298.
- [36] Q. Zhang, L. Gao, F. Li, et al., *Nanoscale* 15 (2023) 5158–5166.
- [37] L. He, X. Yu, R. Huang, et al., *Nano Today* 42 (2022) 101334.
- [38] L. Zhu, Z. Lu, L. Zhang, et al., *Chin. Chem. Lett.* 33 (2022) 2491–2495.
- [39] R. Huang, L. He, S. Li, et al., *Nanoscale* 12 (2020) 2445–2451.
- [40] Z. Yang, D. She, C. Sun, et al., *Anal. Methods* 14 (2022) 1534–1539.
- [41] J. Zhu, W. Sun, Y. Yao, et al., *Anal. Chim. Acta* 1267 (2023) 341322.
- [42] Z. Lu, Y. Shi, Y. Ma, et al., *Anal. Chem.* 94 (2022) 9466–9471.
- [43] S. Xing, Z. Lu, Q. Huang, et al., *Theranostics* 10 (2020) 10262–10273.
- [44] J. Liu, L. Zhang, W. Zeng, et al., *Chin. Chem. Lett.* 34 (2023) 108141.
- [45] S. Liu, X.L. He, T. Zhang, et al., *Chin. Chem. Lett.* 33 (2022) 1933–1935.
- [46] X. Dong, J. Chi, L. Zheng, et al., *Lab Chip* 19 (2019) 2897–2904.
- [47] L. Zhao, H. Wang, J. Fu, et al., *Biosens. Bioelectron.* 214 (2022) 114487.
- [48] Q. Wang, L. Zou, X. Yang, et al., *Biosens. Bioelectron.* 135 (2019) 129–136.
- [49] N. Bellasai, R. D'Agata, V. Jungbluth, et al., *Front. Chem.* 7 (2019) 570.
- [50] B. Lin, T. Tian, Y. Lu, et al., *Angew. Chem. Int. Ed.* 60 (2021) 7582–7586.
- [51] H. Chen, X. Ma, X. Zhang, et al., *Chin. Chem. Lett.* 34 (2023) 107701.
- [52] Y. Yu, W.S. Zhang, Y. Guo, et al., *Biosens. Bioelectron.* 167 (2020) 112482.
- [53] J. Zhou, C.X. Zhang, C.C. Hu, *Chin. Chem. Lett.* 35 (2024) 109561.
- [54] L. Zhao, R.J. Sun, P. He, et al., *Anal. Chem.* 91 (2019) 14773–14779.
- [55] M. Lin, Y. Chen, S. Zhao, et al., *Angew. Chem. Int. Ed.* 61 (2022) e202116932.
- [56] Z. Guo, B. Jin, Y. Fang, et al., *Chin. Chem. Lett.* 33 (2022) 4208–4212.